Lightning Damage Testing of Aircraft Composite-Reinforced Panels and Its Metal Protection Structures

Fusheng Wang [1,2,*], **Xiangteng Ma [1,2]**, **Yao Zhang [1,2]** and **Senqing Jia [1,2]**

[1]   School of Mechanics, Civil Engineering and Architecture, Northwestern Polytechnical University, Xi'an 710129, China; maxiangteng1992@163.com (X.M.); zhangyao2016@mail.nwpu.edu.cn (Y.Z.); sqjia@mail.nwpu.edu.cn (S.J.)
[2]   Institute of Structural Health Montoring and Control, Northwestern Polytechnical University, Xi'an 710129, China
*   Correspondence: fswang@nwpu.edu.cn; Tel.: +86-29-8843-1000

check for updates

Featured Application: This work has a potential application to anti-lightning-strike design of aircraft carbon fiber/epoxy composite panels.

Abstract: In order to investigate the lightning damage behavior of an aircraft carbon fiber/epoxy composite-reinforced panel and its protection structures, four types of panels were selected to carry out a lightning experiment. Panels were without protection, with a full-sprayed aluminum coating, a local-sprayed aluminum coating, and a full-embedded copper mesh filling, respectively. Their surface and internal damage was detected via ultrasonic C-scanning. Results showed delamination damage for the protected and unprotected specimens due to substantial lightning Joule heat, thermal shock, and internal explosion. The aluminum coatings and the copper mesh had good shielding performance against anti-lightning strike damage. The protection method with a full-sprayed aluminum coating is more effective compared with the other two methods. This study is valuable to investigate the protection effectiveness of metal covers when aircraft composite structures are struck by lightning.

Keywords: lightning strikes; composite panel; metal protection; delamination damage; ultrasonic C-scanning

1. Introduction

Aircraft carbon fiber/epoxy composite materials are insulated and more likely to be damaged by lightning strikes due to their high anisotropic electrical and thermal conductivity. Lightning discharge on composite materials can result in direct physical damage effects such as ablation, erosion, explosion, structural distortion, and strength degradation, influencing aircraft flight safety [1,2]. Considering the complicated interaction between lightning plasma channels and composite structures, the damage mechanism has been studied through experiment and simulation methods. For example, the lightning damage process of composite laminates has been simulated through the coupled electrical-thermal numerical method [3–5]. Additionally, coupled thermal-electrical coupled analysis combined with the element deletion technique has also been used to evaluate the lighting ablation damage behavior of composite laminate and its protection structures in our previous study [6,7]. Although numerical simulation can be used as an auxiliary method, lightning experiment verification and relative damage testing is indispensable for investigating damage behavior of carbon fiber/epoxy composite materials and their protection structures.

Lightning experiments are aimed at collecting response information of composite structures exposed to lightning strikes for the development of lightning protection systems. The defect and damage characteristics of composite materials can be evaluated by non-destructive testing methods such as ultrasonic testing, X-ray inspection, optical method, and thermal wave testing [8]. For example, lightning experiments of both pristine composite specimens and specimens with stainless steel fasteners have been carried out by a simulated generator, with which the damage degree and pattern is tested via ultrasonic scanning and optical microscopy [9]. An artificial lightning experiment was also performed to investigate lightning damage behavior of graphite/epoxy composite laminates and concluded that lightning parameters, such as peak current, electrical charge, and action integral of lightning current waveform, greatly influence composite damage, the degree and pattern of which visual inspection, ultrasonic scanning, micro X-ray inspection, and sectional observation is used to test [10]. Available research shows that lightning strikes can induce fiber breakage, matrix cracking, and delamination accompanied with ablation and thermal decomposition under the thermal shock of supersonic plasma.

At present, methods of lightning strike protection for aircraft composites include metal mesh or foil bonded with resin, metal or metalized fibers bonded with resin, and polymer-based film or conductive adhesives [11]. Considering the expense, lightning strike protection is generally achieved by covering conductive metals on composite surface such as the sprayed aluminum coating and embedded copper mesh filling. In addition, carbon nanofibers also have excellent electrical conductivity and thermal properties, which have a great potential application in aircraft lightning protection engineering [12]. When carbon nanofiber paper mingled with nickel nanostrands covers the composite surface, research shows that electrical conductivity plays an important role in reducing composite lightning damage [13]. Although these lightning protection strategies are effective, lightning damage to composite specimens is unavoidable. For the damaged carbon fiber/epoxy composite specimens with the embedded copper mesh filling, structural and electrical integrity can be reestablished to some extent by the bonded scarf repair with the embedded copper mesh filling, in which the damage area is overlapped by composite repair to reconnect the path of electrical conductivity [14].

In order to investigate the lightning damage behavior of T700/BA9916 carbon fiber/epoxy composite-reinforced panel and its protection structures, lightning experiments were carried out, and an ideal current waveform was adopted to simulate natural lighting strikes. Ultrasonic C-scanning technique was used to detect their damage pattern, especially for composite delamination damage. Four different structural types are selected: without protection, with a full-sprayed aluminum coating, with a local-sprayed aluminum coating, and with a full-embedded copper mesh filling, respectively.

2. Experiment and Testing Procedure

The aircraft composite-reinforced panel is shown in Figure 1. The thickness of the composite panel and the T-type stiffener was 3.6 mm and 24 ply. The length and width of the composite panel were 500 and 250 mm, respectively. The width and height of the stiffener were 50 and 38 mm, respectively. The lay-ups of composite-reinforced panel are shown in Figure 2, and details are given in Table 1. The thickness of the left and right T-type stiffeners was 1.8 mm at 12 ply. The reinforced core was filled into the R zone. The J-116B film adhesive was located between the composite panel and the T-type stiffener. Three types of lightning protection structures for composite-reinforced panel are shown in Figure 3. The composite-reinforced panel without protection was used as a benchmark specimen. For composite panels with full- and local-sprayed aluminum coatings, a 0.2 mm aluminum layer thickness was considered. For the composite panel with a copper mesh filling, a 0.2 mm copper mesh thickness was considered, and the space between meshes was 0.1 mm.
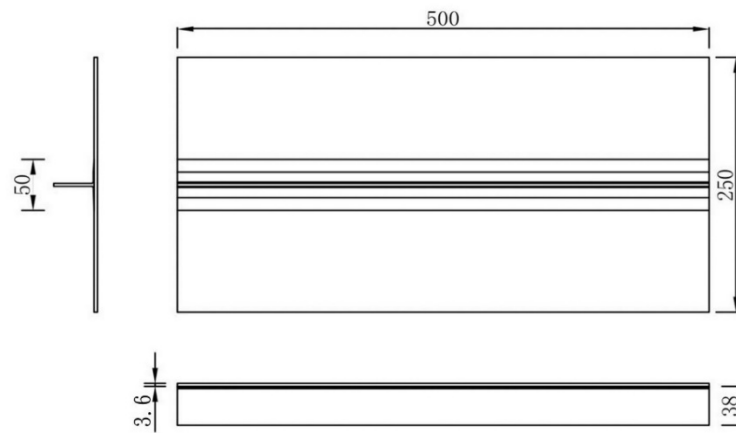
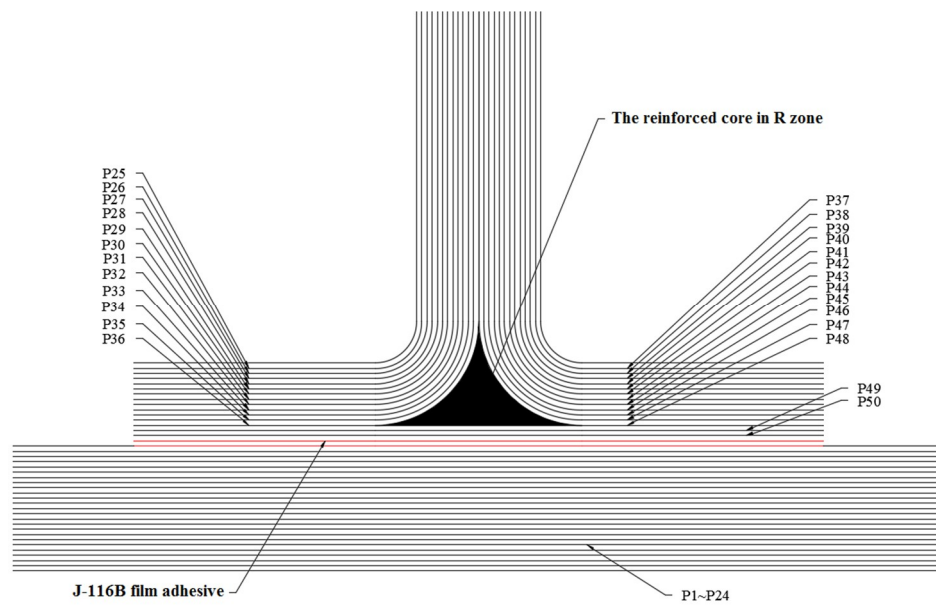**Figure 1.** The aircraft composite-reinforced panel (unit: mm).

Figure 2. Lay-up profile of composite-reinforced panel.

Table 1. Lay-ups of the composite-reinforced panel.

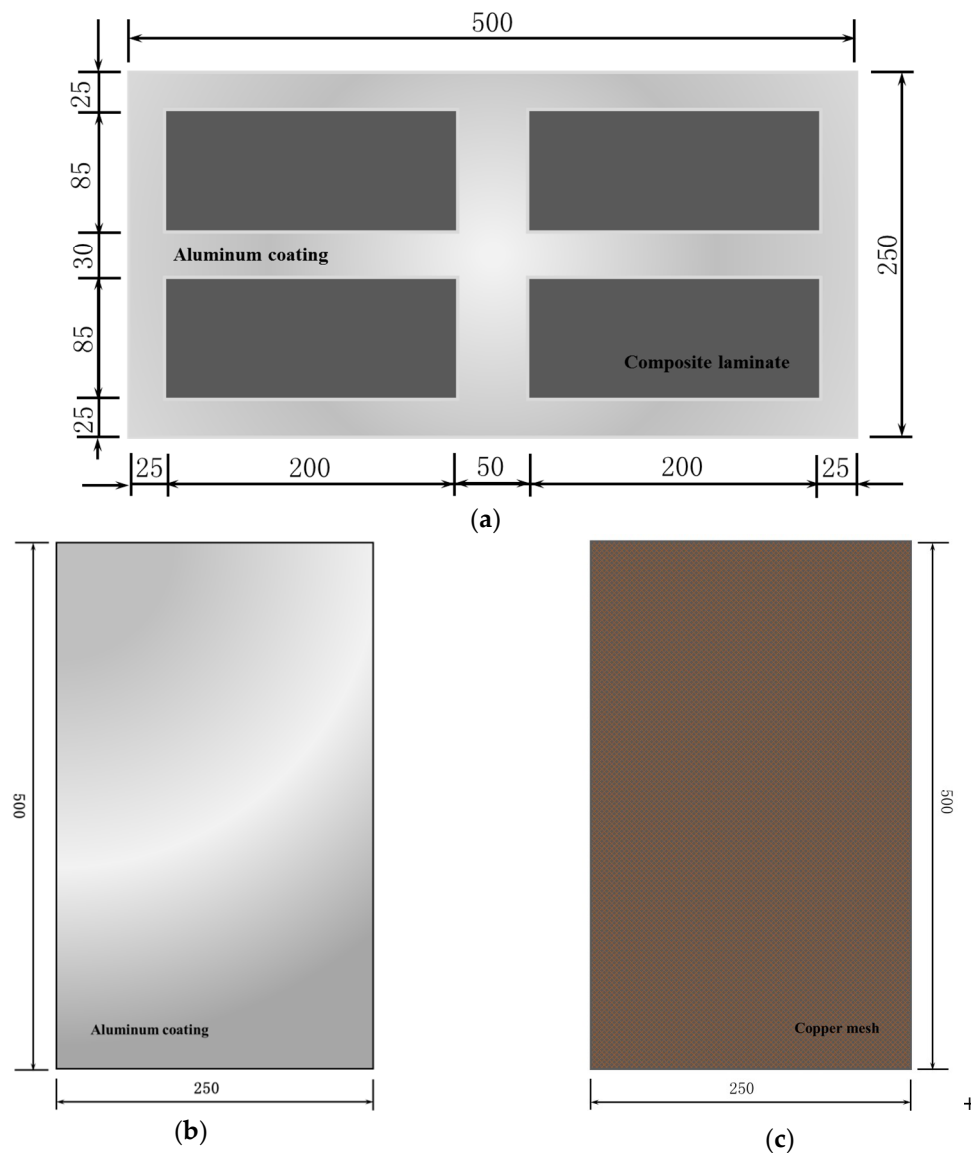| Lay-Up of Composite Panel		Left Lay-Up of T-type Stiffener		Right Lay-Up of T-type Stiffener		Underneath Lay-Up of T-type Stiffener	
Number		Angle	Number	Angle	Number	Angle	Number	Angle
P1	P24	45	P25	45	P37	−45	P49	45
P2	P23	0	P26	0	P38	0	P50	0
P3	P22	−45	P27	−45	P39	45		
P4	P21	90	P28	0	P40	0		
P5	P20	−45	P29	90	P41	90		
P6	P19	0	P30	0	P42	0		
P7	P18	45	P31	−45	P43	45		
P8	P17	0	P32	0	P44	0		
P9	P16	45	P33	90	P45	90		
P10	P15	90	P34	0	P46	0		
P11	P14	−45	P35	45	P47	-45		
P12	P13	0	P36	0	P48	0		

Figure 3. Three types of lightning protection structures for composite-reinforced panel: (**a**) the local-sprayed aluminum coating; (**b**) the full-sprayed aluminum coating; (**c**) the full-embedded copper mesh filling. (Unit: mm).

According to SAE standards [15–17], the lightning strike experiment was performed by continuously loading impulse electrical current waveforms such as A, B, C, and D to composite-reinforced panels, and the distance between test specimens and electrode was set to 50 mm. A, B, C, and D current waveforms are shown in Figure 4, and their parameters are given in Table 2. Metal strips were placed on the sides of composite specimens, and their ends were linked with ground wire so as to ensure a good ground connection. The atmospheric pressure was 1.013×10^5 Pa, the temperature was 25 °C, and the humidity was 79%. The ultrasonic C-scanning technique shown in Figure 5 is based on the propagation of the high frequency sound wave. The probe is capable of both transmitting and receiving high frequency sound waves, scanning the specimen surface on a certain path, and internal damage information regarding the composite specimen can be obtained by the reflected wave.
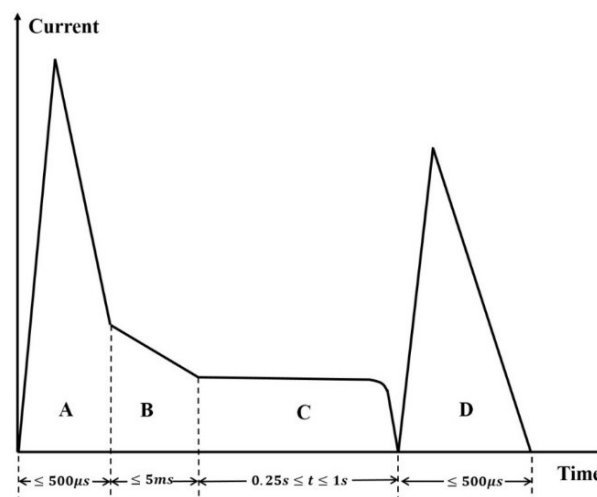
Figure 4. A, B, C, and D current waveforms.

Table 2. Parameters of impulse electrical current waveforms.

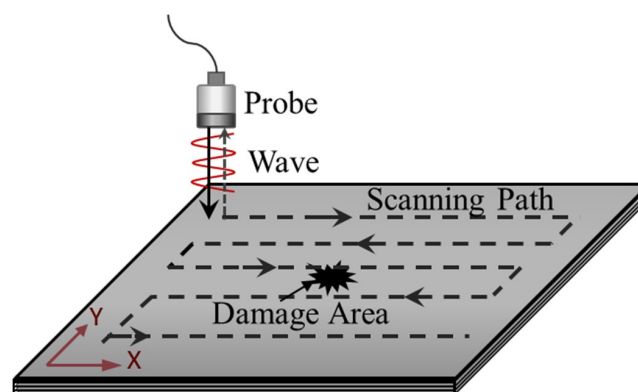| Current Waveform	Peak Current	Average Amplitude	Time Duration	Action Integral	Total Transfer Charge
A	200 kA ± 10%	—	340 ± 40 μs	1.8×10^6 A^{2}s ± 20%	—
B	—	2 kA ± 20%	5 ms ± 10%	—	10 C ± 10%
C	—	200 A ± 10%	1 s	—	200 C ± 20%
D	100 kA ± 10%	—	190 ± 50 μs	0.25×10^6 A^{2}s ± 20%	—

Figure 5. The ultrasonic C-scanning process.

The composite-reinforced panels were immersed in water. The damage pattern and degree was detected by a full digital ultrasonic C-scanning system (UPK-T36) with a 5 MHz detector at room temperature. The detector was toward the composite panel and backward stiffener. The specimen surface was selected as the initial scanning location, and each specimen was scanned twice. Firstly, the composite-reinforced panel was scanned entirely in order to roughly distinguish the lightning damage condition. Secondly, further damage conditions were scanned, and the initial scanning point was 0.96 mm, and the scanning thickness was 2.64 mm. The scanning resolution ratio was 0.5 mm, and the range symmetrically involves the main damage region of the composite specimen, the length of which was 390 mm with a 175 m/s velocity and the width of which was 200 mm with a 100 m/s velocity. The scanning blind zone was considered in order to neglect zones on the front detector by setting the delay time of the echo, where invalid echoes may be disturbed to deal with the real echo when its intensity reaches a certain extent. The initial delay time was 75 μs and the scanning time margin was 10 μs along the height direction when the detector time was 0, which indicates that echo data within a 75 and 85 μs delay time are valid, while those with a delay time between 0 and 75 μs or greater than 85 μs are invalid. The initial scanning threshold was a 50% amplitude

of the first maximum reflected wave. The detection threshold was a 1% amplitude of the reflected wave, and this wave was considered background noise when the detection threshold was below 1% amplitude. The above parameters of ultrasonic C-scanning are summarized in Table 3.

Table 3. Parameters of ultrasonic C-scanning.

Parameter	Value	Parameter		Value
Detector	5 MHz	The scanning length	Size	390 mm
			Velocity	175 m/s
Initial scanning point	0.96 mm	The scanning width	Size	200 mm
			Velocity	100 m/s
The scanning thickness	2.64 mm	The scanning time margin		10 μs
The scanning resolution ratio	0.5 mm	Initial scanning threshold		50% amplitude of the first maximum reflected wave
Initial delay time	75 μs	Detection threshold		1% amplitude of the reflected wave

3. Results and Discussion

For the four different types of aircraft carbon fiber/epoxy composite-reinforced panels, the surface damage pattern and size due to lightning strikes is shown in Figure 6. The composite panel without protection was the most serious, caused by fiber fracture and matrix cracking, resin vaporization, delamination, etc. Lightning damage propagated significantly along the fiber direction. For lightning protection structures, lightning strikes can result in the melting of metal covers, and composite damage is inevitable. The melting of the metal coating was propagated outward from the attachment point of the lightning arc. The surface damage area of four different types of composite-reinforced panels is given in Table 4. It can be seen that the surface damage area of the lightning protection structures was larger than that of structures without protection, and the local-sprayed aluminum coating had the largest damage area. Although the metal covers were damaged, the composite-reinforced panels underneath were protected from lightning strikes, and composite damage was decreased to some extent. Therefore, the internal lightning damage state of composite structures under metal covers needs to be further evaluated by non-destructive testing method such as ultrasonic C-scanning in our present study.

Table 4. Surface damage area of composite-reinforced panels.

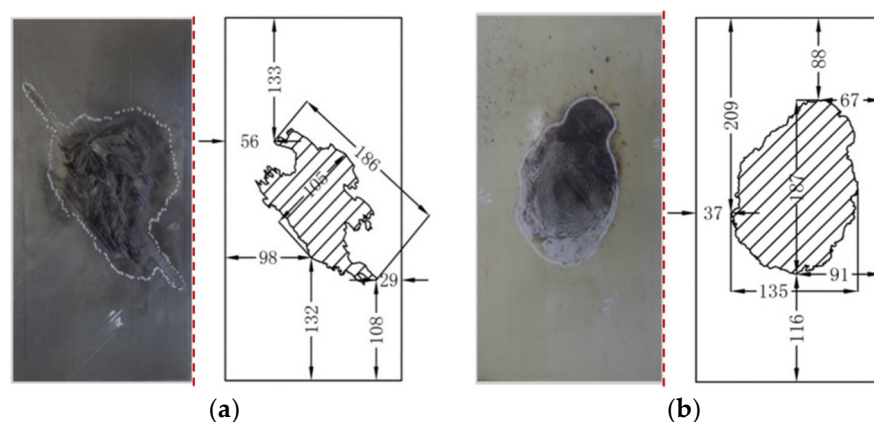|	Structure (a)	Structure (b)	Structure (c)	Structure (d)
Damage area	10,359 mm^2	17,942 mm^2	20,139 mm^2	11,502 mm^2
Percentage	13.28%	23.00%	25.81%	14.75%

(a)
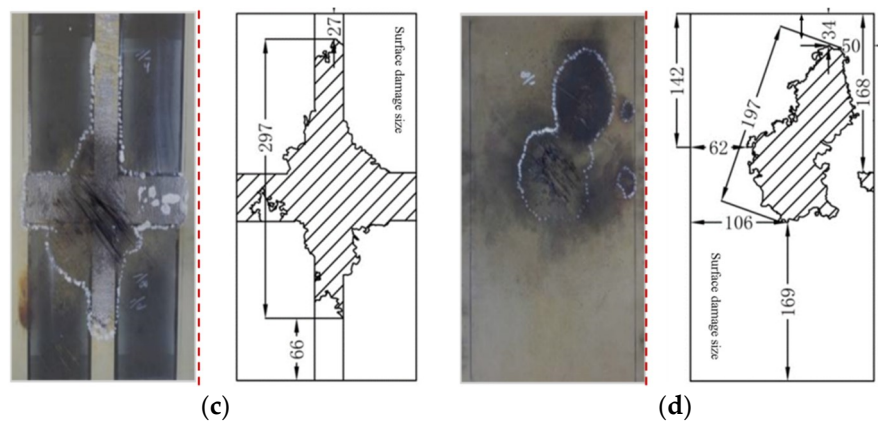
(b)

Figure 6. *Cont.*

Figure 6. Surface damage pattern and size of four different types of composite-reinforced panels: (**a**) composite-reinforced panel without protection; (**b**) composite-reinforced panel with a full-sprayed aluminum coating; (**c**) composite-reinforced panel with a local-sprayed aluminum coating; (**d**) composite-reinforced panel with a full copper mesh filling. (Unit: mm).

Damage echo amplitude, echo location, and location data of the second scanning is shown in Figures 7–10 for four different composite panels—those without protection, with a full-sprayed aluminum coating, with a local-sprayed aluminum coating, and with a full-embedded copper mesh filling, respectively. Delamination damage is developed with a ladder type along the thickness direction due to substantial lightning Joule heat, thermal shock, internal explosion, etc. The higher percentage is, the larger echo the amplitude is and the lower the absorbed energy of the reflected wave is. This implies a lower occurrence probability of delamination damage or internal composite-reinforced panel flaws. The white zone in the echo amplitude figures implies that echo amplitude was beyond the scanning height range or dissipated completely due to the complex damage pattern such as the fluffed damage, which is in accordance with the black zone in the echo location figures. Damage location data were analyzed corresponding to the selected section of the test specimen, presented in yellow cross curves.

Part of the central lightning attachment zone is shown in white and red in Figure 7a. Vast surface carbon fibers were fractured or sublimated, and appeared to have unconstrained conditions, and an epoxy resin matrix had a carbonized decomposition based on visible detection. The white and red zones distributed along the 45 degree fiber direction on the top lamina and a narrow fiber fracture belt ran throughout the entire specimen, which is symmetrical with respect to the attachment point of impulse electrical current. An approximate elliptical damage appeared irregularly around the white and red zones, and was mainly formed in the deterioration zone. Delamination damage is distinguished by abrupt color changes in Figure 7b. Damage location data in Figure 7c show that the specimen surface was slightly tilted and that the deterioration depth was about 2 mm apart from the top lamina.

Approximate circular attachment damage appears irregularly in the central zone in Figure 8a, in which a small part is presented in white and the other in red. The reason may be that the thickness of the sprayed aluminum coating is not constant along the specimen surface due to the spraying craft limit, which results in a non-uniform electrical charge distribution. The isotropic aluminum layer was uniformly distributed, and electrical current was conducted along its surface. Comparison with visible detection shows that the aluminum layer was intensely melted and vaporized in the central zone. Many carbon fibers were broken up, and the epoxy resin matrix had carbonized decomposition in this zone. Figure 8b further shows the damage zone, presented in red and black, and was used to assess delamination damage. The white damage spot on the lower composite panel shown in Figure 8a, which corresponds to the black spot shown in Figure 8b, might have been produced by the broken carbon fibers and carbonized resin matrix. Damage location data in Figure 8c show that the specimen surface was tilted slightly and that the deterioration depth was about 1.8 mm apart from the top lamina. The yellow zone in Figure 8c, when

comparing it with that in Figure 8b, shows that delamination damage may have appeared. The green might correspond to the red carbonized damage zone shown in Figure 8b.
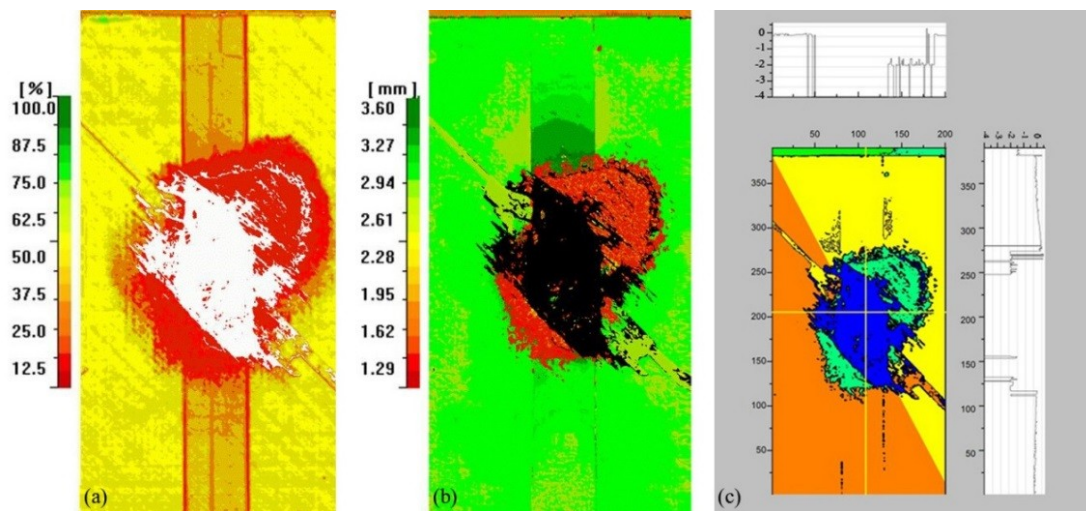

Figure 7. Echo amplitude, echo location, and location data for composite-reinforced panel without protection: (**a**) echo amplitude; (**b**) echo location; (**c**) location data (Unit: mm).
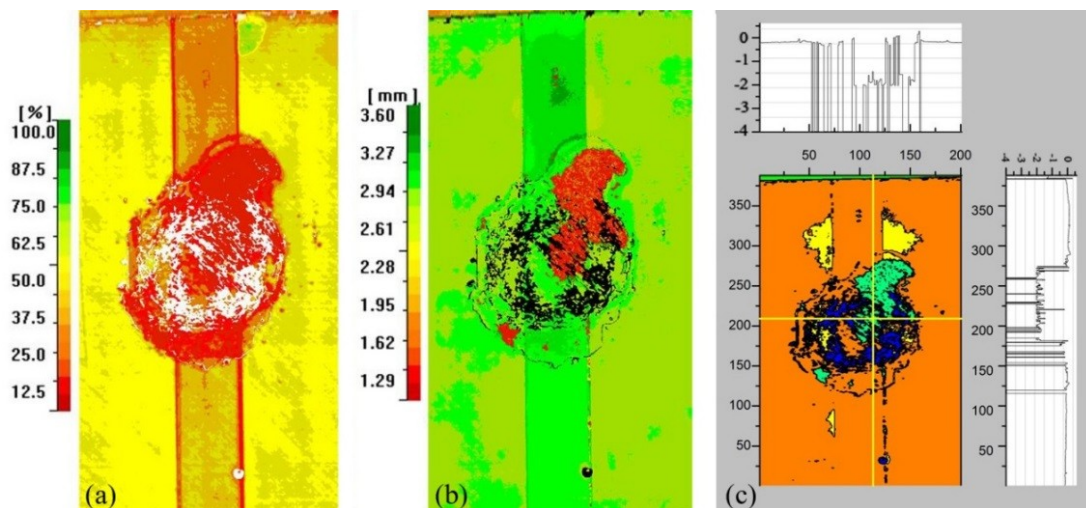

Figure 8. Echo amplitude, echo location, and location data for composite-reinforced panel with a full-sprayed aluminum coating: (**a**) echo amplitude; (**b**) echo location; (**c**) location data (Unit: mm).

The lightning electrical current was a priority to conduct along the aluminum layer direction. Attachment damage mainly appears in the cross-shaped sprayed aluminum zone in Figure 9a, distributed along the 45 degree fiber direction on the top central lamina, which is presented in white and red, and the area around this zone is presented in yellow. Comparison with visible detection shows that the aluminum layer in the damage zone was also melted and vaporized, carbon fibers were broken up, and the epoxy resin matrix had carbonized decomposition in part on the sprayed aluminum coating and in part on the aluminum zone without spraying. It can be seen in Figure 9b that there is an irregular red zone along the 45 degree direction on the top central lamina, where the fiber fracture belt does not run throughout the whole specimen, which implies that not only does the surface specimen appear to have a fiber fracture but the internal specimen also has carbonized deterioration. Delamination damage was assessed by the obvious change in color in Figure 9b. Damage location data in Figure 9c show that the deterioration depth was about 1.8 mm apart from the top lamina.
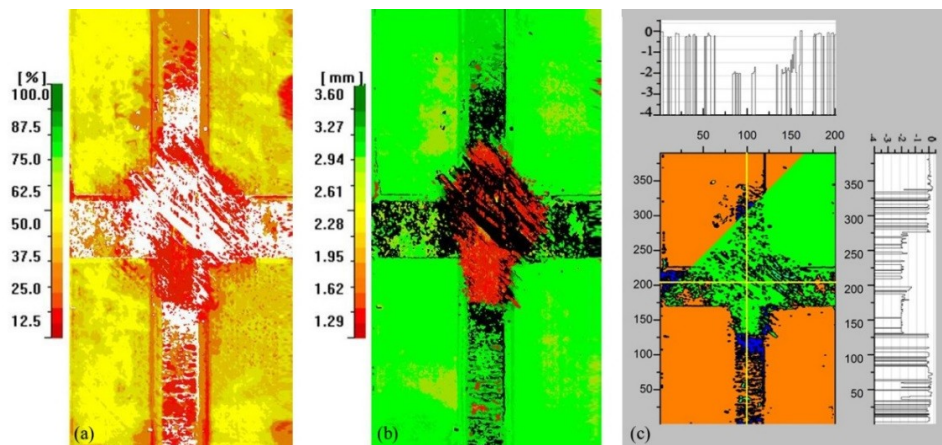
Figure 9. Echo amplitude, echo location, and location data for composite-reinforced panel with a local-sprayed aluminum coating: (**a**) echo amplitude; (**b**) echo location; (**c**) location data (Unit: mm).

Both elliptical lightning attachment damage zones mainly appear in the center and top right corners in Figure 10a, which are connected and presented in white and red, and the area around these zones is presented in yellow. It was easy to induce and accumulate an electrical charge on the specimen surface with the coarse copper mesh, and this charge resulted in point discharge. Comparison with visible detection shows that the copper mesh in the damage zone was broken up, melted, and vaporized. A large number of carbon fibers were fractured, and the epoxy resin matrix had carbonized decomposition. Part of the damage zone was distributed with multiple irregular spots. The yellow zone might have been produced by the oxidized copper mesh, which was peeled off of the surface specimen. More of the damage zone of the broken carbon fibers and carbonized resin matrix is shown in Figure 10b, presented in red and black, was used to assess delamination damage. The red spots shown in Figure 10b correspond to the orange spots shown in Figure 10a and can be seen on the lower surface composite panel, where the copper mesh was not oxidized or peeled off. The center point of different irregular concentric circles, inherent flaws and lightning damage, is presented in a different color. The latter might have been produced when lightning impulse electrical currents were conducted along the copper mesh and entered the composite panel to release energy at this location. Damage location data in Figure 10c show that the surface specimen was slightly tilted and the deterioration depth was about 1.8 mm apart from the top lamina. It can be seen that the lightning damage zone in Figure 10c presented in blue corresponds to that in Figure 10b presented in black.
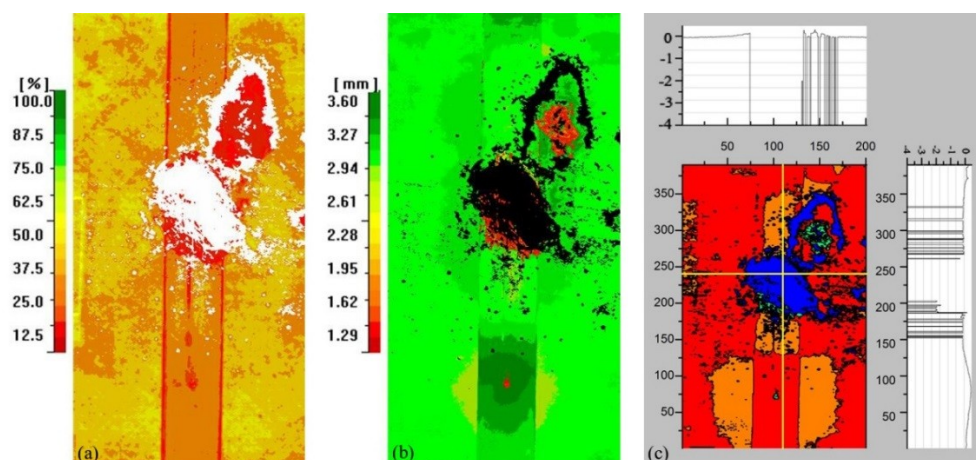

Figure 10. Echo amplitude, echo location and location data for composite-reinforced panel with full copper mesh filling: (**a**) echo amplitude; (**b**) echo location; (**c**) location data (Unit: mm).

As a whole, delamination damage was developed with a ladder type along the thickness direction due to substantial lightning Joule heat, thermal shock, internal explosion, etc. The specimen with full-sprayed aluminum protection was more effective, although surface damage size was larger compared with the specimens with no protection and full copper mesh filling protection. The above analysis shows that the surface damage of the specimen with full-sprayed aluminum protection mainly comes into being by the melted aluminum layer when electrical currents are conducted along that layer. Based on ultrasonic C-scanning results analysis, there is a lower amount of lightning damage to composite-reinforced panels with full-sprayed aluminum coatings. Therefore, the full-sprayed aluminum protection can well prevent composite-reinforced panels from lightning strike damage. However, regarding aircraft weight loss, such composite-reinforced panels will be heavier than those with local-sprayed aluminum protection. Future work will place emphasis on the theoretical study of protection effects on damage quality, such as the damaged area and the maximum damage thickness due to lightning strikes in composite-reinforced panels, especially by the numerical simulation method, as was performed in previously published papers [6,7].

4. Conclusions

Against a background of anti-lightning-strike aircraft carbon fiber/epoxy composites, a lightning strike experiment was carried out, and full digital ultrasonic C-scanning was used to investigate the damage behavior of composite-reinforced panel and its protection structures after lightning strikes. The following main conclusions can be drawn.

1. Lightning impulse electrical currents are conducted mainly along the fiber direction of the unprotected carbon fiber/epoxy composite-reinforced panel that has maximum electrical conductivity. The protected specimens in favor of lightning current conduction show improved anti-lightning damage performance compared with the unprotected specimen.
2. Delamination damage occurred in protected and unprotected specimens, and might have extended to the stiffener. Overall, the specimen with full-sprayed aluminum protection was more effective than those with local-sprayed aluminum and full copper mesh filling protection in terms of anti-lightning delamination damage, although the deterioration damage depth was almost the same.

At present, the above study has been applied to the anti-lightning-strike design of carbon fiber/epoxy composite panels in civil aircraft. However, it should be noted that ultrasonic C-scanning is more effective for detecting composite delamination damage. In further investigations, other non-destructive testing auxiliary systems should be further investigated to deeply detect composite damage behavior due to lightning strikes, such as fiber breakage and matrix cracking.

Author Contributions: Material testing and formal analysis: F.W., X.M., Y.Z. and S.J.; Formal analysis and writing—original draft preparation: F.W.

References

1. Fisher, F.A.; Plumer, J.A.; Perala, R.A. *Aircraft Lightning Protection Handbook*; Lightning Technologies Inc.: Pittsfield, MA, USA, 1989.
2. Rupke, E. *Lightning Direct Effects Handbook*; Lightning Technologies Inc.: Pittsfield, MA, USA, 2002.
3. Ogasawara, T.; Hirano, Y.; Yoshimura, A. Coupled thermal–electrical analysis for carbon fiber/epoxy composites exposed to simulated lightning current. *Compos. Part A Appl. Sci. Manuf.* **2010**, *41*, 973–981. [CrossRef]

4. Abdelal, G.; Murphy, A. Nonlinear numerical modelling of lightning strike effect on composite panels with temperature dependent material properties. *Compos. Struct.* **2014**, *109*, 268–278. [CrossRef]

5. Muñoz, R.; Delgado, S.; González, C.; López-Romano, B.; Wang, D.-Y.; LLorca, J. Modeling lightning impact thermo-mechanical damage on composite materials. *Appl. Compos. Mater.* **2014**, *21*, 149–164. [CrossRef]

6. Wang, F.S.; Ding, N.; Liu, Z.Q.; Ji, Y.Y.; Yue, Z.F. Ablation damage characteristic and residual strength prediction of carbon fiber/epoxy composite suffered from lightning strike. *Compos. Struct.* **2014**, *117*, 222–233. [CrossRef]

7. Wang, F.S.; Ji, Y.Y.; Yu, X.S.; Chen, H.; Yue, Z.F. Ablation damage assessment of aircraft carbon fiber/epoxy composite and its protection structures suffered from lightning strike. *Compos. Struct.* **2016**, *145*, 226–241. [CrossRef]

8. Garnier, C.; Pastor, M.-L.; Eyma, F.; Lorrain, B. The detection of aeronautical defects in situ on composite structures using non destructive testing. *Compos. Struct.* **2011**, *93*, 1328–1336. [CrossRef]

9. Feraboli, P.; Miller, M. Damage resistance and tolerance of carbon/epoxy composite coupons subjected to simulated lightning strike. *Compos. Part A* **2009**, *40*, 954–967. [CrossRef]

10. Hirano, Y.; Katsumata, S.; Iwahori, Y.; Todoroki, A. Artificial lightning testing on graphite/epoxy composite laminate. *Compos. Part A* **2010**, *41*, 1461–1470. [CrossRef]

11. Gagné, M.; Therriault, D. Lightning strike protection of composites. *Prog. Aerosp. Sci.* **2014**, *64*, 1–16. [CrossRef]

12. Kim, H.M.; Kim, K.; Lee, C.Y.; Joo, J.; Cho, S.J.; Yoon, H.S.; Pejaković, D.A.; Yoo, J.W.; Epstein, A.J. Electrical conductivity and electromagnetic interference shielding of multiwalled carbon nanotube composites containing Fe catalyst. *Appl. Phys. Lett.* **2004**, *84*, 589–591. [CrossRef]

13. Gou, J.; Tang, Y.; Liang, F.; Zhao, Z.; Firsich, D.; Fielding, J. Carbon nanofiber paper for lightning strike protection of composite materials. *Compos. Part B Eng.* **2010**, *41*, 192–198. [CrossRef]

14. Kawakami, H.; Feraboli, P. Lightning strike damage resistance and tolerance of scarf-repaired mesh-protected carbon fiber composites. *Compos. Part A Appl. Sci. Manuf.* **2011**, *42*, 1247–1262. [CrossRef]

15. *Aircraft Lightning Zoning*; Aerospace Recommended Practice APP 5414; SAE: Warrendale, PA, USA; Troy, MI, USA, 2005.

16. *Aircraft Lightning Environment and Related Test Waveforms*; Aerospace Recommended Practice ARP 5412; SAE: Warrendale, PA, USA; Troy, MI, USA, 2005.

17. *Aircraft Lightning Test Methods*; Aerospace Recommended Practice ARP 5416; SAE: Warrendale, PA, USA; Troy, MI, USA, 2005.